Diversification across biomes in a continental lizard radiation.

Abstract

Ecological opportunity is a powerful driver of evolutionary diversification, and predicts rapid lineage and phenotypic diversification following colonisation of competitor-free habitats. Alternatively, topographic or environmental heterogeneity could be key to generating and sustaining diversity. We explore these hypotheses in a widespread lineage of Australian lizards: the *Gehyra variegata* group. This clade occurs across two biomes: the Australian monsoonal tropics (AMT), where it overlaps a separate, larger bodied clade of *Gehyra* and is largely restricted to rocks; and in the larger Australian arid zone (AAZ) where it has no congeners and occupies trees and rocks. New phylogenomic data and coalescent analyses of AAZ taxa resolve lineages and their relationships and reveal high diversity in the western AAZ (Pilbara region). The AMT and AAZ radiations represent separate radiations with no difference in speciation rates. Most taxa occur on rocks, with small geographic ranges relative to widespread generalist taxa across the vast central AAZ. Rock-dwelling and generalist taxa differ morphologically, but only the lineage-poor central AAZ taxa have accelerated evolution. This accords with increasing evidence that lineage and morphological diversity are poorly correlated, and suggests environmental heterogeneity and refugial dynamics have been more important than ecological release in elevating lineage diversity.

Keywords: Australian Arid Zone, cryptic species, Australian Monsoonal Tropics, *Gehyra*, non-ecological diversification, phylogenomics

Introduction

Ecological opportunity, where lineages gain access to underexploited or empty niche space, may lead to elevated rates of phenotypic evolution and lineage diversification (Lack 1947; Schluter 2000). This is perhaps best demonstrated in radiations that have occurred subsequent to colonisation of biotically impoverished islands (Lack 1947; Gavrilets and Losos 2009). However, it is increasingly clear that major radiations can occur without a corresponding acceleration of ecological and morphological divergence, often described as non-adaptive or non-ecological radiation (Gillespie 2009; Rundell and Price 2009). This is especially likely to occur across isolated but relatively stable habitats, which provide few changes in selection that would drive morphological divergence, but where lineages persist in isolation for long enough to allow genetic divergences to accumulate (Kozak et al. 2006; Singhal and Moritz 2013). Even in classic adaptive radiations, considerable speciation occurs within ecomorphs, suggesting that across many radiations the relationship between ecological and lineage diversification may be indirect or weak (Glor et al. 2003; Losos et al. 2006; Blom et al. 2016). Hence, an alternative to ecological release is that diversity of radiations is shaped primarily by topographic complexity, through promoting allopatric or parapatric speciation, opportunity for niche partitioning, and persistence in refugia through oscillating climates (Moritz et al. 2000; Kozak et al. 2006; Smith et al. 2014; Badgley et al. 2017).

Tests for adaptive radiation require highly resolved phylogenies coupled with phenotypic and ecological data across contrasting systems (e.g., Schluter 2000; Poe et al. 2018). Increasing evidence of morphologically cryptic taxa (Bickford et al. 2007; Pérez-Ponce de León and Poulin 2016; Struck et al. 2018) raises the possibility that studies using current taxonomy have underestimated the number of evolutionarily independent lineages as units of analysis. If so, the relative importance of processes such as isolation and allopatric

speciation that generate lineages, but are not linked to overt phenotypic variation, may also be underestimated (Purvis 2008). Building from typical mtDNA phylogeography, large-scale multilocus data combined with coalescent-based analytical methods provide the means to identify evolutionarily distinctive, yet morphologically cryptic, lineages (Fujita et al. 2012; Moritz et al. 2018), and incorporate them into analyses of diversification dynamics; however, the extent to which such units represent transient metapopulations rather than species remains an open question (Carstens et al. 2013; Sukumaran and Knowles 2017).

Here we use a phylogenomic approach to robustly identify lineages, resolve their relationships and test for effects of ecological release vs. topographic heterogeneity in a widespread and diverse continental clade of scansorial lizards: the "*variegata* group" of *Gehyra* geckos. This is a monophyletic clade of 21 species (Sistrom et al. 2009; Doughty et al. 2012; Hutchinson et al. 2014; Bourke et al. 2017; Doughty et al. 2018) within the broader genus *Gehyra*; however, phylogeographic analyses indicate that the true number of species could be twice this (Pepper et al. 2013; Moritz et al. 2018) and many species relationships remain poorly resolved despite considerable effort (Sistrom et al. 2014). The *variegata* group has radiated extensively across the Australian arid zone (AAZ) and monsoonal tropics (AMT) since the Miocene (Heinicke et al. 2011). For the mostly rock-dwelling taxa of the AMT, and using a phylogenomic approach, Moritz et al. (2018) resolved many more lineages than were evident from existing taxonomy (with the more genetically divergent and less cryptic taxa then described; Doughty et al. 2018) and found clear evidence of size partitioning in sympatric assemblages. In the AMT, the *variegata* group co-occurs with another moderately diverse clade of *Gehyra*, the *australis* group (Mitchell 1965). Species in the *australis* group occur on rocks and trees, tend to be substantially larger (65–96 mm vs 40–73 mm), and where they co-occur, the species of the *variegata* group (the *Gehyra nana* clade; Moritz et al. 2018) appear to be excluded from both arboreal habitats and large rock faces (Moritz, Oliver,

75 Doughty unpubl. data). Conversely, across the AAZ the *australis* group is absent, and
76 members of the *variegata* group occur both on rocks (including open faces), and on trees far
77 from rocky habitats (i.e., generalists). An ecological release model would therefore predict
78 that absence of competition from the larger *australis* group species has accelerated both
79 lineage diversification and ecological and phenotypic evolution of the *variegata* group in the
80 AAZ relative to the AMT.

81 The alternative view is that genetic isolation and divergence in climatically and/or
82 ecologically complex regions have played a dominant role in generating diversity. While both
83 the AMT and AAZ have extensive rocky ranges and plateaus with associated *Gehyra*, this
84 key habitat is more disjunct in the relatively larger AAZ (both in terms of distance, and the
85 lack of suitable intervening habitat), potentially increasing the probability of localised
86 divergence within and among rocky areas. The AAZ has also experienced extensive
87 expansion and spread of sand dunes and retreat of woodlands since the mid-Pliocene (Fujioka
88 et al. 2009), which may have further isolated key rocky habitats in this biome. These complex
89 and ancient ranges and plateaus are also expected to have acted as major arid zone refugia
90 through the climatic oscillations of the Neogene (Morton et al. 1995; Byrne et al. 2008). In
91 support of this hypothesis, topographically complex ranges of the Pilbara and Central
92 Uplands show both deeply divergent range-restricted paleoendemic lineages, and finely
93 structured intraregional phylogeography (Oliver et al. 2010; Pepper et al. 2011; Pepper et al.
94 2013; Oliver and McDonald 2016). The topographic complexity hypothesis predicts that
95 lineage diversity in the *variegata* group will be highest in complex ranges and plateaus, but
96 with rates higher in the AAZ than the AMT.

97 Here, to explore how the *variegata* group has diversified across biomes, we first use
98 phylogenomics using custom exon capture (Bi et al. 2012; Bragg et al. 2016; Jones and Good
99 2016) to resolve independent lineages and their relationships using concatenation and species

tree methods, as already done for the AMT taxa by Moritz et al. (2018). We then test for differences in patterns and rates of both lineage diversification and phenotypic evolution across biomes (the AAZ and AMT), regions (Pilbara, central AAZ, and AMT), and habitats (rock and generalist). These analyses find that lineage diversity and breadth of habitat use are both higher in the AAZ; however, rates of diversification and phenotypic evolution do not differ between biomes, except for an elevated rate of phenotypic evolution in the central AAZ. Across all biomes most lineages are associated with rocky habitats, especially complex refugial areas, and these rock-dwellers have much smaller ranges than generalist taxa. These results point to topographic complexity, rather than ecological release, having a dominant role in diversification, with isolated rocky ranges promoting localised divergence and persistence.

Materials and Methods

Our strategy for sampling, sequencing, bioinformatics, delimitation, and phylogenetic analysis is shown in Fig. S1. We first identified evolutionarily independent lineages within the 11 currently recognised arid zone species of the *variegata* group, applying both discovery and validation methods to extensive exon sequence data. We then added representatives of previously delineated lineages from the *nana* clade, a monophyletic radiation of nine species and 12 lineages that represents the AMT members of the *variegata* group (Doughty et al. 2018; Moritz et al. 2018). We further included two outgroups from the *australis* group of *Gehyra*, and estimated the phylogeny of the resulting 44 taxa using concatenation, and both summary and full Bayesian species tree estimation approaches. Interpretation of phylogenetic relationships was based primarily on a larger dataset (547 loci with at least 90% taxa) with

concatenation and summary species tree approaches. Given computational limits, the full Bayesian coalescent species tree method StarBEAST2 (Ogilvie et al. 2017) was applied to a subset of the data (106 loci with at least 95% taxa), but even so the size of the dataset required a newly developed hierarchical approach (see below). Because concatenation can substantially overestimate tip lengths in recent radiations (Ogilvie et al. 2016), with possible downstream effects on rate analyses, we used the StarBEAST2 tree for subsequent analyses of ancestral states and rates of diversification and morphological evolution (Fig. S2).

SAMPLE SELECTION AND SEQUENCING FOR ARID ZONE TAXA

Based on prior analyses of mtDNA phylogeography (Sistrom et al. 2009; Pepper et al. 2013; Doughty unpubl. data), we sampled 30 candidate lineages across 11 recognised species in the AAZ, generating exon capture data for 64 individuals (Fig. 1; Table S1). Sequences from *G. spheniscus* and *G. xenopus*, AMT rock-dwelling species, were not available; otherwise, sampling of known species and component lineages of the *variegata* group is complete. The exon capture probes we used targeted four commonly used phylogenetics genes (*BDNF*, *C-mos*, *PDC*, and *RAG1*) and 1716 other protein coding exon regions developed from *G. nana* (Bragg et al. 2017) and *G. oceanica* (Tonione et al. 2016) transcriptomes. The target regions were identified on the basis of a reciprocal best BLAST (Altschul et al. 1990) hit to an exon from the *Anolis* genome (Alfoldi et al. 2011; accessed in Ensembl release 67, Flicek et al. 2013), and were >200 bp in length. Probes were designed against target exons and synthesised as a SeqCap EZ NimbleGen in-solution capture system. Previous studies have demonstrated that such probes are highly effective for target enrichment across clades considerably older than *Gehyra* (Bragg et al. 2016). The pooled sample library was hybridised to these probes and amplified by ligation-mediated PCR using the SeqCap EZ Developer Library (NimbleGen) protocol, modified to include the alternative blocking

oligonucleotides detailed in Peñalba et al. (2014). A quantitative PCR was run on aliquots of both pre- and post-hybridisation libraries, to ensure the hybridisation reaction had amplified the two target primers but not the non-target control (as per Bi et al. 2012). The successful post-hybridisation library was sequenced using 100 bp paired-end sequencing on an Illumina HiSeq2000 system at the Biomolecular Resource Facility, John Curtin School of Medical Research, Australian National University.

BIOINFORMATIC WORKFLOW

Raw sequencing reads were cleaned and trimmed using a workflow described by Singhal (2013) which was distributed with the SCPP pipeline (*pre-cleanup* and *scrubReads* scripts; Peñalba et al. 2014), using *E. coli* (K12 MG1655; Blattner et al. 1997) and human (GRCh37; Ensembl release 67) genome sequences as contaminant references. Cleaned reads were assembled into contigs using a pipeline described by Bragg et al. (2016) (see Supporting Information Methods 1.1 for further details). The assembled AAZ haplotype sequences were combined with 28 representative orthologous haplotypes from the AMT *nana* clade (Moritz et al. 2018), and two *australis* group outgroups (Fig. 1; Table S1). Sequences of each locus were aligned using MACSE v. 1.2 (Ranwez et al. 2011) and trimmed (full details in Supporting Information Methods 1.1). To reduce the non-random distribution of missing data, we only kept alignments that contained at least 90% of samples, yielding 547 loci.

LINEAGE IDENTIFICATION AND PHYLOGENETIC ANALYSES

We applied discovery and validation methods to detect evolutionary independent lineages among AAZ specimens using the exon sequence data. For discovery, we used tr2 (Fujisawa et al. 2016), which assesses observed vs. expected rates of gene tree congruence under coalescent theory for rooted triplets of candidate taxa and a specified guide tree. We used

sequence data (a single haplotype for 64 individuals, 1–4 different individuals per candidate lineage) and RAxML gene trees for 499 exons with >90% complete data, using the RAxML concatenated phylogeny as a guide tree (see Summary species tree analysis, below). To validate the candidate lineages (deep mtDNA phylogeographic clades) within species, we also used BPP v. 3.2 (Yang 2015). Because of computational limits, we selected the 100 longest loci from the above exons and applied BPP to candidate lineages within each of six monophyletic AAZ clades within the *variegata* group (Table S2). Priors were set to small ancestral population sizes (theta: G(2, 2000)) and shallow divergence times (tau: G(2, 2000)), following Leaché and Fujita (2010). Two independent analyses (different starting seeds) were performed for each clade, adjusting the fine-tuning parameters so that acceptance proportions lay between 0.15–0.70; the burn-in was set to 10,000, sampling every five iterations for a total of 500,000 generations.

Concatenation analysis

The haplotype sequences from the refined MACSE alignments (547 loci, with a minimum of 90% of samples per locus) were concatenated using FASconCAT v. 1.0 (Kück and Meusemann 2010). We conducted a search for the best-fit substitution model with IQ-TREE v. 1.4.4 (Nguyen et al. 2015) using the option "–m TESTONLY". The resulting model (GTR+I+G) was then used in RAxML v. 8.2.8 (Stamatakis 2014) to search for the best-scoring Maximum Likelihood (ML) tree and perform a rapid bootstrap analysis with 100 replicates. Convergence was assessed *a posteriori* using the “bootstopping” criterion (Pattengale et al. 2010).

Summary species tree analysis

The same dataset of 547 loci was used to estimate 499 gene trees (best of 10 replicates; 48 "invariant" loci removed) and 499 bootstrap trees (100 bootstrap replicates each) for one haplotype per individual with RAxML (GTR+I+G model of substitution, model optimisation precision set to 0.0001). These were then used as input trees in a summary multispecies coalescent analysis, estimating the species tree topology (from multiple individuals per species; branch lengths are arbitrary) using ASTRAL-II v. 4.8.0 with multilocus bootstrapping (Mirarab and Warnow 2015).

Divide and conquer StarBEAST2 analysis

After setting up some simpler exploratory analyses in BEAUTi, we added R scripts to BEASTmasteR (Matzke 2015; Matzke and Wright 2016) to set up StarBEAST2 analyses. We used the algorithms implemented in BEAST2 (Bouckaert et al. 2014; Drummond and Bouckaert 2015), as StarBEAST2 v. 0.13.1 (Ogilvie et al. 2017). All Excel settings files, R code, and XML files are available at https://github.com/nmatzke/Ashman_etal_Gehyra. From the original MACSE alignment, we randomly selected 106 loci that satisfied criteria appropriate for a StarBEAST2 analysis (200–500 bp, sequences at least 90% complete alignments and with at least 95% taxa, no paralogs). We selected two haplotypes (from different specimens) per taxon, and partitioned by codon position (shared across all loci) under strict clock and HKY+G models. All runs were conducted for 1 billion generations, and examined in Tracer v. 1.6 for convergence. The run length was sufficient to obtain ESS >200 for virtually all parameters (usually >1500).

To overcome the computational limits on numbers of individuals, we employed a "divide and conquer" strategy (*sensu* Antonelli et al. 2017). We identified strongly supported subclades with many closely related lineages from initial RAxML and ASTRAL trees, and removed them for smaller, subclade-specific StarBEAST2 analyses (full details in Supporting

Information Methods 1.2). When a subclade was removed, at least two lineages delimiting the subclade were kept to represent the subclade's root node; any lineages that were phylogenetically isolated, or had highly uncertain placement, were also left in the remaining "skeleton tree" (Fig. S3). We dated the skeleton tree by assigning a crown age of the combined *australis* and *variegata* groups at 13.2–26.0 Mya, based on a fossil calibrated phylogeny spanning geckos (Gamble et al. 2015; Oliver et al. 2017): we used a Normal prior (mean = 19.1, standard deviation = 3.3).

After the subclades were removed, the dated skeleton tree was estimated with StarBEAST2. The StarBEAST2 analyses on each subclade were given only a relative date prior (the subclade root node had a tight prior of Normal (1,0.001)). After the StarBEAST2 analyses had completed, the trees sampled from the posterior of each subclade analysis were integrated with trees sampled from the posterior of the skeleton tree analysis, by replacing each pair of subclade-delimiting lineages with a sampled full subclade tree, with branch lengths scaled to match the subclade root date of the sampled skeleton tree. The new collection of dated trees contained all lineages and was treated (with caveats) as a posterior distribution of dated species trees, and summarised as a Maximum Clade Credibility tree calculated with TreeAnnotator.

MACROEVOLUTIONARY ANALYSES

To visualise and understand patterns of lineage and phenotypic diversification across biomes we undertook analyses of ancestral state, diversification rates, and morphological evolution as summarised in Fig. S2. Using the StarBEAST2 tree, we ran three ancestral state analyses, and tested for differences in diversification rate and morphology across biomes, regions and habitats. We also calculated the gamma statistic (which tests for deviations from a constant-

rate, pure-birth diversification model) in R using the APE v. 3.5 function *gammaStat* (Paradis et al. 2004; R Core Development Team 2015).

Ancestral state estimation

Ancestral states for geographic range, biome, and habitat were estimated using BioGeoBEARS v. 0.2.2–2 (Matzke 2013a). Geographic distributions were discretised into three broad areas: the Australian Monsoonal Tropics ("M"); and two from the AAZ, the Pilbara region to the west ("P"), including the Pilbara and adjacent Ashburton ranges to the south; and central Australia ("C"), covering the arid regions of eastern WA, Northern Territory, Queensland, and South Australia. Some species lived in both the central and Pilbara regions; none lived in all three. Species' biome was discretised into either "AAZ" or "AMT" (coded as "D" and "W", for "dry" and "wet"). Species' habitat was categorised as "rock" ("R") or "generalist" ("T" for "tree") and is based on the authors' extensive field experience, habitat records for specimens in the WAM, and summaries in field guides (Wilson and Swan 2013; Cogger 2014). This coding captures broad distributional patterns rather than absolute microhabitat usage, and there are some ambiguities for species that are plastic in foraging habitat. By our classification, rock-dwellers are frequently found foraging on vegetation as well as rocks, but never occur away from rocky ranges which provide refuge sites during the day. By contrast, generalists are rarely found on rocks, and occur in habitats far removed from rocky ranges. As *G. pilbara* (a termite mound specialist) is rarely observed on trees and occurs primarily in the rocky Pilbara ranges, we classify it as a rock-dweller in these analyses. By contrast, *G. kimberleyi* is common on termite mounds and is also found on trees or rocks, but occurs in areas with no rocks, so is classified here as a generalist.

Six standard biogeographical models (Matzke 2013b) were run on the geographic range dataset in BioGeoBEARS: DEC (Ree et al. 2008); DIVALIKE, a likelihood

interpretation of DIVA (Ronquist 1997), and BAYAREALIKE, a likelihood interpretation of BayArea (Landis et al. 2013). Three additional "+J" models were added, which use the free parameter *j* to model the relative weight of founder-event speciation at cladogenesis (Matzke 2014). The maximum range size was set to three. The six basic biogeographic models were also run on the biome and habitat datasets. In addition, a Markov-*k* model (M*k*; Lewis 2001) was run on these two datasets; the model is constructed in BioGeoBEARS by editing the default DEC model by fixing the parameters *d*, e, and *j* to 0, setting the parameter *a* (for anagenetic range-switching) to be free, and eliminating from the state space the null range and any ranges made up of more than one area. Models were fit using maximum likelihood, and the fit was compared with AICc model weights (Burnham and Anderson 2002). Ancestral state estimates were made under each model.

Comparisons of diversification rates

Following Jetz et al. (2012) and R scripts from Harvey et al. (2017), we calculated the diversification rate (DR) statistic for each tip, which is a summary statistic of the speciation rate derived from the inverse of the branch lengths (i.e., number of splitting events) leading to the particular tip on the tree. We used phylogenetic generalised least squares (PGLS) in the R package CAPER v. 0.5.2 (Orme 2013) to test for differences in the log-transformed DR statistic between biogeographic regions (AMT, central AAZ, Pilbara), biomes (AAZ vs. AMT), or habitats (rock vs. generalist).

Estimation of range sizes

To estimate approximate range sizes for taxa, we collated location records from the Atlas of Living Australia for unambiguously recognisable species, from recently published revisions (Hutchinson et al. 2014; Doughty et al. 2018), and genetically verified records from the

298 Western Australian Museum (Kealley et al. in press) and the Moritz lab (Moritz unpubl.
299 data). We then used minimum convex polygons to estimate range size using ArcGIS v. 10.4
300 (ESRI 2016).
301
302 Morphological evolution analyses
303 Over 500 adult *variegata* group specimens were measured for 11 traits (Table S3; full details
304 in Supporting Information Methods 1.3). We used samples that were assigned to lineages
305 based on mtDNA (*ND2*) sequences or, for lineages with few genotyped specimens, using
306 diagnostic morphological characters by P. Doughty and M. Hutchinson (Table S4). Sexual
307 dimorphism was tested with multivariate analysis of covariance (MANCOVA, sex = fixed
308 effect); no significant differences were found (Wilks' lambda = 0.85, $F = 1.05$, $p = 0.41$), so
309 male and female measurements were pooled. Statistical analyses were performed on the log-
310 transformed intra-lineage averages of each trait, using the R packages Picante v. 1.6–2,
311 Phytools v. 0.5–38, GEIGER v. 2.0.3 and NLME v. 3.1–122 (Kembel et al. 2010; Revell
312 2012; Pennell et al. 2014; Pinheiro et al. 2015).
313 Non-phylogenetic principal component analyses (PCAs) were performed using the
314 morphological traits, both uncorrected and corrected for body size (for the latter, using
315 residuals calculated from linear regressions of body shape traits against SVL). The PCAs
316 were visualised using phylomorphospace plots (Phytools; Revell 2012). Phylogenetic signal
317 was assessed for morphological traits and principal components (PCs) with Blomberg's K
318 (Blomberg et al. 2003). Both phylogenetic (Phytools) and non-phylogenetic one-way
319 analyses of variance (ANOVA) were used on the major PCs to compare morphology among
320 lineages, with habitat (rock vs. generalist) or biome (AAZ vs. AMT) as the explanatory
321 factor. Patterns of variation across regions (AMT, central AAZ, Pilbara), habitat, and biome
322 were further examined for body shape traits heavily loaded on PC axes, using PGLS with

body size and ecological factors as predictors, under the model of evolution that best fitted each trait (Brownian motion or Ornstein-Uhlenbeck; selected by lowest AICc score).

Morphological variance (disparity) across lineages was compared, using the *morphol.disparity* function of Geomorph v. 3.0.1 (Adams and Otárola-Castillo 2013) on size-corrected traits. The function calculates the morphological variance for each biome group from the covariance matrix, and compares them to 999 random permutations of disparity under a linear model to obtain a test statistic (absolute difference in variances). The rates of morphological evolution (size-corrected traits) were analysed across biomes (AAZ vs. AMT), regions (AMT, central AAZ, Pilbara) and habitat types (rock vs. generalist), using the *compare.evol.rates* function. The evolutionary rates of two variable and habitat-relevant traits, body size and size-corrected snout depth, were also analysed by comparing log likelihoods of single and multiple rate BM models of continuous trait evolution using the *mvBM* function in mvMORPH v. 1.0.8 (Clavel et al. 2015).

Results

LINEAGE RELATIONSHIPS, DIVERSITY, RANGE SIZES, AND ANCESTRAL STATES

The RAxML concatenated tree (547 loci; Fig. 2A) and ASTRAL species tree (499 loci; Fig. 2B) analyses identify three strongly supported major clades within the *variegata* group: (i) *lazelli-pulingka* (rocky ranges in the AAZ), (ii) *nana* clade (AMT), and (iii) a diverse AAZ clade. Relationships among these three major clades are not well resolved with either RAxML or ASTRAL. Within the AAZ clade, the Australian Central Uplands endemic taxon *G. moritzi* is a divergent sister group to the remainder ("main AAZ clade"), which has five

groups: (a) *purpurascens-einasleighensis*, (b) *variegataC1-2*, (c) the *punctata B* clade, (d) the *punctata A* clade, and (e) the *variegata* clade. These five groups are supported across both methods, albeit with lower support for (a) and (b) from ASTRAL. The 106 loci StarBEAST2 species tree (Fig. 3) differs from the concatenated and ASTRAL species trees in having the *nana* clade branching off first (albeit with weak support), and in confidently (pp = 0.99) grouping the long-branch taxon *G. moritzi* with the other divergent AAZ species, *G. pulingka* and *G. lazelli*. All analyses infer that *G. punctata* and *G. variegata* are polyphyletic as currently construed (full details in Supporting Information Results 1.1).

The number of supported lineages across the whole *variegata* group is double the number of recognised species (40 lineages from 20 species; see Fig. S4, Table S2 and Supporting Information Results 1.2 for full details) despite recent taxonomic revisions of some components (Hutchinson et al. 2014; Doughty et al. 2018). There are 27 lineages in the AAZ and 13 in the AMT, of which 32 are limited to rocky areas and eight are habitat generalists. Lineage diversity is especially high within the nominal species *G. variegata* (six lineages) and *G. punctata* (11 lineages). While recognising the need for further sampling and analysis of some problematic taxa (especially *G. montium* and the *G. variegata B* lineages), we treat all 40 inferred lineages as separate taxa for subsequent analyses of diversification and morphological evolution. As found by Sistrom et al. (2012), the large-bodied population *G. lazelliLP* was not distinct genetically, although we treat it as distinct from *G. lazelli* for morphological analyses.

The high diversity of lineages within the ranges and plateaus of the Pilbara (western AAZ) is especially notable (Fig. 4A). As a corollary, average range sizes for the Pilbara and AMT taxa are 18-fold less than for the central AAZ taxa (Pilbara: 57,846 km^2; AMT: 58,052 km^2; central AAZ: 930,901 km^2; Table S5). The Pilbara also has more taxa that meet the

372 definition of short-range endemics (<10,000 km^2; Harvey 2002): nine in the Pilbara, three in
373 the AMT and three in the central AAZ.

374 Using the StarBEAST2 tree, the BioGeoBEARS analysis (AMT, central AAZ,
375 Pilbara) finds that the most credible model is DEC (Table S6). The ancestral range for the
376 widespread arid zone radiation, and also the whole *variegata* group, is ambiguous (Fig. 4A;
377 similar to the uncertainty of relationships at the base of the *variegata* group). However,
378 independent histories of the central AAZ taxa are highlighted, with a restricted-range,
379 paleoendemic rock-dwelling group (*G. moritzi*, *G. lazelli*, *G. pulingka*) contrasting with the
380 recently (Plio–Pleistocene) derived and geographically widespread *G. minuta-versicolor*
381 clade. The latter is evidently derived recently from the Pilbara radiation. For biomes (AMT
382 vs. AAZ; Fig. 4B), the M*k* model is the best fit (Table S7). The ancestral biome of the
383 *variegata* group is most likely the AAZ. Late Miocene origins are inferred for the initial
384 divergence of all three major groups *(lazelli-pulingka-moritzi*, the AMT *nana* clade and the
385 main AAZ clade). For the habitats (rock vs. generalist; Fig. 4C), the M*k* model is again the
386 best fit (Table S8) and rock-dwelling is inferred to be ancestral, with multiple independent
387 shifts to generalist habitat use in the AAZ clades, and just one in the AMT (with the latter
388 shift in a lineage that occurs at the boundary of the AMT and AAZ).
389
390 **RATES OF DIVERSIFICATION**
391 Diversification rates are estimated to decrease over time based on the mean gamma statistic (-
392 2.85, from 100 sampled trees; Fig. S5). The DR statistic (tip speciation rate) ranged from
393 0.098 (*G. moritzi*) to 0.676 lineages/My (*G. versicolor*), with a mean of 0.301 lineages/My
394 (Table 1). The PGLS analyses found no significant differences in the DR statistic between the
395 biomes (AAZ vs. AMT), biogeographic regions (AMT, central AAZ, Pilbara), or habitat
396 types (rock vs. generalist).

MORPHOLOGICAL EVOLUTION

In the PCA on all traits ("sPCA"), the first PC axis (sPC1; body size) explains 91% of the variation (loading strongly and negatively with all traits; Table S9). Body size varies substantially within several clades; e.g., the *nana* (40–59 mm), *purpurascens-einasleighensis* (37–55 mm), and *punctata B* (41–65 mm) clades (circled in Fig. 5A). There is significant phylogenetic signal for sPC1 (Blomberg's $K = 0.44$, $p = 0.049$), although no significant effect of either habitat or biome on body size.

In the PCA on the size-corrected body shape traits ("rPCA"), the first three PC axes explain 73% of the variation, loading with all head traits and foreleg length (Fig. 5A–C; Table S9). While rPC1 has no significant phylogenetic signal, rPC2–3 and the majority of the trait measurements do have phylogenetic signal (Table S10). The first two rPCA axes show no significant relationship with habitat or biome. However, on the rPC3 axis (snout depth), rock-dwelling lineages have significantly lower values (Fig. 5C) than the generalist lineages (phylogenetic ANOVA: $F = 13.65$, $p = 0.006$). Additionally, the termite mound specialist *G. pilbara* has an unusually short head and snout (rPC1; circled in Fig. 5A). Like the other axes, there is no significant difference in rPC3 values between the AAZ and the AMT.

For individual morphological traits, only head and snout depth are significantly associated with habitat, with rock-dwellers having shallower heads/snouts than generalists (PGLS: head depth $T = 2.89$, $p = 0.007$; snout depth $T = 4.46$, $p < 0.001$; Fig. 6). None of the PC loading traits (head/legs) differ significantly between biomes or biogeographic regions (Table S11). Removing the termite mound specialist *G. pilbara* from the analyses does not cause any qualitative changes to the results (data not shown).

There are no significant differences in morphological disparity between habitats, regions, or biomes. Similarly, there is no significant difference in morphological evolution

rates between biomes or habitats. However, when considered by region, the central AAZ lineages have a significantly higher rate of morphological evolution than the AMT lineages (observed rate ratio = 2.01, $p = 0.044$; Table 1). When focusing on individual traits (body size and snout depth), there is no support for differences in morphological evolution rates between the two biomes (AAZ and AMT) or between habitats (rock and generalist; Table S12). However again, when considered by region, the central AAZ taxa have a significantly higher rate of body size evolution than the other two regions (log likelihood of multiple rate model >2 greater than single rate model; Table S12), but snout depth is not significant.

Discussion

We set out to test the hypothesis that the AAZ taxa of the *variegata* group of *Gehyra* would show increased rates of diversification and morphological evolution relative to their AMT sister clade, reflecting either (i) expansion of habitat to trees as well as rocks (in the absence of larger *australis* group species), or (ii) the larger size of this biome and more disjunct nature of key rocky habitats within it. Applying a phylogenomic approach, together with morphological analyses, we found twice as many lineages as described species, largely resolved their relationships, and revealed that generalist taxa have deeper heads than the rock-dwelling taxa. The western AAZ, centred on the Pilbara which is a major arid zone refugium, has especially high lineage diversity with smaller geographic ranges per taxon. We also found that the AAZ shows evidence for more shifts between rock and generalist ecologies, and the central AAZ has a higher rate of morphological evolution (body size and shape) than the AMT. However, there was no significant difference in diversification rates across the biomes, regions, or habitats.

PATTERNS AND RATES OF LINEAGE DIVERSITY

Resolving the diversity and relationships of lineages in the *G. variegata* group has previously proved intractable, despite the use of karyotypic, allozyme, morphological, mtDNA, and small-scale nuclear datasets (King 1979; Moritz 1986, 1992; Heinicke et al. 2011; Sistrom et al. 2013; Sistrom et al. 2014). As for the AMT *nana* clade (Moritz et al. 2018), the much-improved resolution and largely consistent estimates of phylogeny for the AAZ radiation of *Gehyra* emphasise the value of phylogenomic datasets with comprehensive sampling of taxa for resolving the diversity of radiating taxa (Blom et al. 2017).

Biogeographic analyses indicate that there has been relatively little movement between biomes, a pattern that contrasts with several other co-distributed lineages (Fujita et al. 2010; Oliver et al. 2014a; Brennan and Oliver 2017). Habitat use appears to be more plastic, with several shifts between rocks and trees (generalists) inferred in the main AAZ clade. One shift into generalist habitat use in the far southern (arid) edge of the AMT is also inferred, on the edge of the distribution of the *australis* group, providing further evidence that throughout most of the AMT the *variegata* group has been excluded from trees. While our date estimates are derived from secondary calibrations, they also suggest the main AAZ and the AMT radiations both occurred around the late Miocene, with declining diversification rates. Crown ages for many geographically overlapping radiations in the AMT and AAZ are similar (Oliver and Bauer 2011; Crisp and Cook 2013; Laver et al. 2017), suggesting a common response to increased aridity and seasonality from the late Miocene to the early Pliocene (Martin 2006; Byrne et al. 2008; Sniderman et al. 2016; Christensen et al. 2017).

We found no evidence that lineage diversification rates differ across the AMT, Pilbara, or central AAZ. However, the profusion of small-range lineages in the Pilbara (both rock and generalist) and in the central AAZ ranges (rock only) contrasts against the wide

distribution of generalist species in central AAZ. In the western AAZ, the hyperdiverse and paraphyletic *G. punctata* lineages are associated with the geologically complex Pilbara region, as are several short-range endemic *G. variegata B* and *C* lineages (Fig. 1). Several central AAZ lineages (*G. lazelli*, *G. pulingka* and *G. moritzi*) that are restricted to the Flinders and Central Ranges are paleoendemics that have persisted through multiple cycles of aridification.

In other gecko radiations in Australia (Pepper et al. 2011; Oliver et al. 2014c) and southern Africa (Heinicke et al. 2017), saxicoline lineages also show higher diversity and smaller ranges than more ecologically generalised relatives. In the *variegata* group, we also found that the lineage-rich Pilbara region was likely to be a source of generalist taxa that are now widespread across the central AAZ, suggesting recolonisation of arid woodlands from rocky refugia. In general, the absence of accelerated diversification in the AAZ and the concentration of large numbers of small-range lineages in rocky refugia in both biomes (Moritz et al. 2018) are inconsistent with a model of ecological release, and instead point to the overriding importance of topographic complexity in shaping this radiation.

MORPHOLOGICAL EVOLUTION

Body size is a common axis of ecological diversification in squamate radiations (e.g., Burbrink et al. 2012; Garcia-Porta and Ord 2013; Oliver et al. 2014b). Likewise, in *Gehyra* the main axis of morphological evolution was for body size, although within the *variegata* group this did not vary systematically across biomes or habitats, despite the absence of larger bodied *australis* group species in the AAZ. Previous studies of *variegata* group species also found lability in body size but overall conservatism in body shape (King 1979; Sistrom et al. 2012). In the rock-dwelling *nana* clade, there appears to be displacement of body size in relation to geographically varying patterns of sympatry among lineages (Doughty et al. 2012,

2018; Moritz et al. 2018); the same could be true for the geographically overlapping *punctata B* (mostly large-bodied) and *punctata A* (mostly small-bodied) clades in the Pilbara region, but this remains to be tested.

Taxa closely associated with rocks had significantly shallower heads and snouts than generalists. Studies of other lizards have found that dorsoventral flattening of rock-dwellers is the most consistent difference across habitat types (Revell et al. 2007; Goodman and Isaac 2008). This body shape is probably beneficial both biomechanically (keeping the centre of mass close to the rock face; Aerts et al. 2003) and ecologically (enabling use of narrow crevices for shelter; Vitt et al. 1997). The two *Gehyra* ecomorphs do not differ in leg length, unlike *Anolis* and Australian *Cryptoblepharus* skinks, which have more strikingly divergent ecomorphs (Losos 2009; Blom et al. 2016).

The only other putative ecomorphological pattern we detected involved *G. pilbara,* which has a dramatically shortened head and snout relative to the rest of the *variegata* group (rPC1 outlier; circled in Fig. 5A). *Gehyra pilbara* is the only *Gehyra* species found almost exclusively on termite mounds (Wilson and Swan 2013), suggesting it is a termite-eating specialist, although *G. kimberleyi* also occurs on termite mounds (as well as trees) and was until recently placed in this taxon (Oliver et al. 2016). Other termite-eating specialist geckos in the AAZ (genus *Diplodactylus, Rhynchoedura*; Pianka and Pianka 1976), also appear to have shortened snouts (Storr et al. 1990). Stayton (2005) demonstrated that insectivorous iguanids and agamids converged on short jaws, implying more powerful muscles; a shorter snout may make it easier to catch and quickly consume small prey.

The main result from the morphological analyses is simply that a diverse continental radiation of 40 lineages, with obvious divergence in habitat use and widespread sympatry, shows little signal of predictable patterns of body size evolution linked to ecology, and only weak or idiosyncratic signals for body shape. This contrasts with many of the best examples

of adaptive radiation, especially in lizards, which show great phenotypic diversity and clear links between phenotype and ecology (Losos 2009; Blom et al. 2016). It also contrasts with observations that at shallower phylogenetic scales, *Gehyra* show considerable plasticity in morphology and ecology (Doughty et al. 2012; Sistrom et al. 2012; Moritz et al. 2018). The capacity to undergo rapid microevolutionary shifts apparently does not always translate into marked, or predictable, macroevolutionary patterns. In the case of *Gehyra*, it may be that the generalised scansorial phenotype works well across tree and rock microhabitats. Indeed, many *Gehyra* that use the rocks as permanent retreats also make extensive use of nearby vegetation when foraging (personal observations).

Genetic and morphological diversification in the *variegata* group do not appear to be closely linked. Most strikingly, we find evidence of elevated rates of phenotypic evolution in the region with the lowest lineage diversity: the central AAZ (nine lineages), perhaps driven by the closely related species *G. versicolor* (medium-sized generalist) and *G. minuta* (small rock-dweller). Rates of overall phenotypic evolution otherwise do not differ across habitats or major biomes. Taxa in young, unstable and climatically challenging habitats may show elevated rates of phenotypic evolution (Schluter 2000); hence recent waves of intense aridification, contraction of key habitats (Fujioka et al. 2009), and the presence of comparatively few stable rocky refugia, may underpin higher rates of phenotypic evolution in the central AAZ.

In contrast, in other more geographically complex and climatically buffered regions such as the AMT and Pilbara, any signature of ecophenotypic diversification may be overridden by the proliferation and long-term persistence of localised, divergent, yet ecologically equivalent lineages in refugia (Oliver et al. 2010). Furthermore, aside from rapid and recent shifts in body size that might reflect competitive interactions (Doughty et al. 2012; Sistrom et al. 2012; Hutchinson et al. 2014; Moritz et al. 2018), the overall morphological

diversity in *Gehyra* is limited, and is mostly associated with small shifts in head shape between habitats (deeper heads in generalists, and a shortened snout in the termite mound-dweller).

An "uncoupling" between genetic and phenotypic diversity has been observed in other diverse continental lizard radiations: Hipsley et al. (2014) found an inverse relationship between species richness and morphological diversity in lacertid lizards, and Rabosky et al. (2014) demonstrated a marked reduction in morphological evolutionary rate in the rapidly diversifying *Ctenotus* clade of Australian AAZ skinks. Even in the famous island radiation of *Anolis* lizards, while insular phenotypes are more predictable, they do not show overall greater trait variation than their mainland counterparts (Yoder et al. 2010). While overt adaptive radiations on insular systems have attracted wide attention, there is increasing evidence that in many radiations, especially on continental systems, allopatric processes, combined with relatively subtle morphological shifts, variation in physiology, landscapes, and climate, are often more than sufficient to mediate extensive diversification (Kozak et al. 2006; Garcia-Porta et al. 2017).

References

Adams, D. C. and E. Otárola-Castillo. 2013. geomorph: an r package for the collection and analysis of geometric morphometric shape data. Methods Ecol. Evol. 4:393–399.

Aerts, P., R. Van Damme, K. D'Aout, and B. Vanhooydonck. 2003. Bipedalism in lizards: whole-body modelling reveals a possible spandrel. Proc. R. Soc. B 358:1525–1533.

Alfoldi, J., F. Di Palma, M. Grabherr, C. Williams, L. Kong, E. Mauceli, P. Russell, C. B. Lowe, R. E. Glor, J. D. Jaffe, D. A. Ray, S. Boissinot, A. M. Shedlock, C. Botka, T. A. Castoe, J. K. Colbourne, M. K. Fujita, R. G. Moreno, B. F. ten Hallers, D. Haussler, A. Heger, D. Heiman, D. E. Janes, J. Johnson, P. J. de Jong, M. Y. Koriabine, M. Lara, P. A. Novick, C. L. Organ, S. E. Peach, S. Poe, D. D. Pollock, K. de Queiroz, T. Sanger, S. Searle, J. D. Smith, Z. Smith, R. Swofford, J. Turner-Maier, J. Wade, S. Young, A. Zadissa, S. V. Edwards, T. C. Glenn, C. J. Schneider, J. B. Losos, E. S. Lander, M. Breen, C. P. Ponting, and K. Lindblad-Toh. 2011. The genome of the green anole lizard and a comparative analysis with birds and mammals. Nature 477:587–591.

Altschul, S. F., W. Gish, W. Miller, E. W. Myers, and D. J. Lipman. 1990. Basic local alignment search tool. J. Mol. Biol. 215:403–410.

Antonelli, A., H. Hettling, F. L. Condamine, K. Vos, R. H. Nilsson, M. J. Sanderson, H. Sauquet, R. Scharn, D. Silvestro, M. Töpel, C. D. Bacon, B. Oxelman, and R. A. Vos. 2017. Toward a self-updating platform for estimating rates of speciation and migration, ages, and relationships of taxa. Syst. Biol. 66:152–166.

Badgley, C., T. M. Smiley, R. Terry, E. B. Davis, L. R. G. DeSantis, D. L. Fox, S. S. B. Hopkins, T. Jezkova, M. D. Matocq, N. Matzke, J. L. McGuire, A. Mulch, B. R. Riddle, V. L. Roth, J. X. Samuels, C. A. E. Strömberg, and B. J. Yanites. 2017.

586 Biodiversity and topographic complexity: modern and geohistorical perspectives.
587 Trends Ecol. Evol. 32:211–226.
588 Bi, K., D. Vanderpool, S. Singhal, T. Linderoth, C. Moritz, and J. Good. 2012.
589 Transcriptome-based exon capture enables highly cost-effective comparative genomic
590 data collection at moderate evolutionary scales. BMC Genomics 13:403.
591 Bickford, D., D. J. Lohman, N. S. Sodhi, P. K. L. Ng, R. Meier, K. Winker, K. K. Ingram,
592 and I. Das. 2007. Cryptic species as a window on diversity and conservation. Trends
593 Ecol. Evol. 22:148–155.
594 Blattner, F. R., G. Plunkett, C. A. Bloch, N. T. Perna, V. Burland, M. Riley, J. Collado-
595 Vides, J. D. Glasner, C. K. Rode, G. F. Mayhew, J. Gregor, N. W. Davis, H. A.
596 Kirkpatrick, M. A. Goeden, D. J. Rose, B. Mau, and Y. Shao. 1997. The complete
597 genome sequence of *Escherichia coli* K-12. Science 277:1453–1462.
598 Blom, M. P. K., J. G. Bragg, S. Potter, and C. Moritz. 2017. Accounting for uncertainty in
599 gene tree estimation: summary-coalescent species tree inference in a challenging
600 radiation of Australian lizards. Syst. Biol. 66:352–366.
601 Blom, M. P. K., P. Horner, and C. Moritz. 2016. Convergence across a continent: adaptive
602 diversification in a recent radiation of Australian lizards. Proc. R. Soc. B
603 283:20160181.
604 Blomberg, S. P., T. Garland, and A. R. Ives. 2003. Testing for phylogenetic signal in
605 comparative data: behavioural traits are more labile. Evolution 57:717–745.
606 Bouckaert, R., J. Heled, D. Kühnert, T. Vaughan, C.-H. Wu, D. Xie, M. A. Suchard, A.
607 Rambaut, and A. J. Drummond. 2014. BEAST 2: a software platform for Bayesian
608 Evolutionary analysis. PLoS Comp. Biol. 10:e1003537.

609 Bourke, G., R. C. Pratt, E. Vanderduys, and C. Moritz. 2017. Systematics of a small *Gehyra*
610 (Squamata: Gekkonidae) from the Einasleigh Uplands, Queensland: description of a
611 new range restricted species. Zootaxa 4231:85-99.
612 Bragg, J. G., S. Potter, K. Bi, R. Catullo, S. C. Donnellan, M. D. B. Eldridge, L. Joseph, J. S.
613 Keogh, P. Oliver, K. C. Rowe, and C. Moritz. 2017. Resources for phylogenomic
614 analyses of Australian terrestrial vertebrates. Mol. Ecol. Resour. 17:869–876.
615 Bragg, J. G., S. Potter, K. Bi, and C. Moritz. 2016. Exon capture phylogenomics: efficacy
616 across scales of divergence. Mol. Ecol. Resour. 16:1059–1068.
617 Brennan, I. G. and P. M. Oliver. 2017. Mass turnover and recovery dynamics of a diverse
618 Australian continental radiation. Evolution 71:1352–1365.
619 Burbrink, F. T., X. Chen, E. A. Myers, M. C. Brandley, and R. A. Pyron. 2012. Evidence for
620 determinism in species diversification and contingency in phenotypic evolution
621 during adaptive radiation. Proc. R. Soc. B 279:4817–4826.
622 Burnham, K. P. and D. R. Anderson. 2002. Model selection and multimodel inference: a
623 practical information-theoretic approach. Springer, New York.
624 Byrne, M., D. K. Yeates, L. Joseph, M. Kearney, J. Bowler, M. A. Williams, S. Cooper, S. C.
625 Donnellan, J. S. Keogh, R. Leys, J. Melville, D. J. Murphy, N. Porch, and K. H.
626 Wyrwoll. 2008. Birth of a biome: insights into the assembly and maintenance of the
627 Australian arid zone biota. Mol. Ecol. 17:4398–4417.
628 Carstens, B. C., T. A. Pelletier, N. M. Reid, and J. D. Satler. 2013. How to fail at species
629 delimitation. Mol. Ecol. 22:4369–4383.
630 Christensen, B. A., W. Renema, J. Henderiks, D. de Vleeschouwer, J. Groenveld, I. S.
631 Castaneda, L. Reuning, K. Bogus, G. Auer, T. Ishiwa, C. M. McHugh, S. J.
632 Gallagher, C. S. Fulthorpe, and I. E. Scientists. 2017. Indonesian Throughflow drove

633 Australian climate from humid Pliocene to arid Pleistocene. Geophys. Res. Lett.
634 44:6914–6925.
635 Clavel, J., G. Escarguel, and G. Merceron. 2015. mvMORPH: an R package for fitting
636 multivariate evolutionary models to morphometric data. Methods Ecol. Evol. 6:1311–
637 1319.
638 Cogger, H. 2014. Reptiles and Amphibians of Australia. CSIRO Publishing, Melbourne.
639 Crisp, M. D. and L. G. Cook. 2013. How was the Australian flora assembled over the last 65
640 million years? A molecular phylogenetic perspective. Annu. Rev. Ecol. Evol. Syst.
641 44:303–324.
642 Doughty, P., G. Bourke, L. G. Tedeschi, R. Pratt, P. M. Oliver, R. A. Palmer, and C. Moritz.
643 2018. Species delimitation in the *Gehyra nana* (Squamata: Gekkonidae) complex:
644 cryptic and divergent morphological evolution in the Australian Monsoonal Tropics,
645 with the description of four new species. Zootaxa 4403:201–244.
646 Doughty, P., R. Palmer, M. J. Sistrom, A. M. Bauer, and S. C. Donnellan. 2012. Two new
647 species of *Gehyra* (Squamata: Gekkonidae) geckos from the north-west Kimberley
648 region of Western Australia. Rec. West. Aust. Mus. 27:117–134.
649 Drummond, A. J. and R. R. Bouckaert. 2015. Bayesian evolutionary analysis with BEAST.
650 Cambridge University Press, Cambridge.
651 ESRI. 2016. ArcGIS Desktop. Environmental Systems Research Institute, Redlands, CA.
652 Available at http://desktop.arcgis.com/en/.
653 Flicek, P., M. R. Amode, D. Barrell, K. Beal, K. Billis, S. Brent, D. Carvalho-Silva, P.
654 Clapham, G. Coates, S. Fitzgerald, L. Gil, C. G. Girón, L. Gordon, T. Hourlier, S.
655 Hunt, N. Johnson, T. Juettemann, A. K. Kähäri, S. Keenan, E. Kulesha, F. J. Martin,
656 T. Maurel, W. M. McLaren, D. N. Murphy, R. Nag, B. Overduin, M. Pignatelli, B.
657 Pritchard, E. Pritchard, H. S. Riat, M. Ruffier, D. Sheppard, K. Taylor, A. Thormann,

S. J. Trevanion, A. Vullo, S. P. Wilder, M. Wilson, A. Zadissa, B. L. Aken, E. Birney, F. Cunningham, J. Harrow, J. Herrero, T. J. P. Hubbard, R. Kinsella, M. Muffato, A. Parker, G. Spudich, A. Yates, D. R. Zerbino, and S. M. J. Searle. 2013. Ensembl 2014. Nucleic Acids Res. 42:D749–D755.

Fujioka, T., J. Chappell, L. K. Fifield, and E. J. Rhodes. 2009. Australian desert dune fields initiated with Pliocene–Pleistocene global climatic shift. Geology 37:51–54.

Fujisawa, T., A. Aswad, and T. G. Barraclough. 2016. A rapid and scalable method for multilocus species delimitation using Bayesian model comparison and rooted triplets. Syst. Biol. 65:759–771.

Fujita, M. K., A. D. Leaché, F. T. Burbrink, J. A. McGuire, and C. Moritz. 2012. Coalescent-based species delimitation in an integrative taxonomy. Trends Ecol. Evol. 27:480–488.

Fujita, M. K., J. A. McGuire, S. C. Donnellan, and C. Moritz. 2010. Diversification and persistence at the arid–monsoonal interface: Australia-wide biogeography of the Bynoe's gecko (*Heteronotia binoei*; Gekkonidae). Evolution 64:2293–2314.

Gamble, T., E. Greenbaum, T. R. Jackman, and A. M. Bauer. 2015. Into the light: diurnality has evolved multiple times in geckos. Biol. J. Linn. Soc. 115:896–910.

Garcia-Porta, J. and T. J. Ord. 2013. Key innovations and island colonization as engines of evolutionary diversification: a comparative test with the Australasian diplodactyloid geckos. J. Evol. Biol. 26:2662–2680.

Garcia-Porta, J., M. Simó-Riudalbas, M. Robinson, and S. Carranza. 2017. Diversification in arid mountains: biogeography and cryptic diversity of Pristurus rupestris rupestris in Arabia. J. Biogeogr. 44:1694–1704.

Gavrilets, S. and J. B. Losos. 2009. Adaptive radiation: contrasting theory with data. Science 323:732–737.

683 Gillespie, R. 2009. Adaptive radiation. Pp. 143-152 *in* S. A. Levin, S. R. Carpenter, C.
684 Godfray, A. P. Kinzig, M. Loreau, J. B. Losos, B. Walker, and D. S. Wilcove, eds.
685 The Princeton Guide to Ecology. Princeton University Press, Princeton, NJ.
686 Glor, R. E., J. J. Kolbe, R. Powell, A. Larson, and J. B. Losos. 2003. Phylogenetic analysis of
687 ecological and morphological diversification in Hispaniolan trunk-ground anoles
688 (*Anolis cybotes* group). Evolution 57:2383–2397.
689 Goodman, B. A. and J. L. Isaac. 2008. Convergent body flattening in a clade of tropical rock-
690 using lizards (Scincidae: Lygosominae). Biol. J. Linn. Soc. 94:399–411.
691 Harvey, M. G., G. F. Seeholzer, B. T. Smith, D. L. Rabosky, A. M. Cuervo, and R. T.
692 Brumfield. 2017. Positive association between population genetic differentiation and
693 speciation rates in New World birds. Proceedings of the National Academy of
694 Sciences 114:6328–6333.
695 Harvey, M. S. 2002. Short-range endemism amongst the Australian fauna: some examples
696 from non-marine environments. Invertebr. Syst. 16:555–570.
697 Heinicke, M. P., E. Greenbaum, T. R. Jackman, and A. M. Bauer. 2011. Phylogeny of a
698 trans-Wallacean radiation (Squamata, Gekkonidae, *Gehyra*) supports a single early
699 colonization of Australia. Zool. Scr. 40:584–602.
700 Heinicke, M. P., T. R. Jackman, and A. M. Bauer. 2017. The measure of success: geographic
701 isolation promotes diversification in *Pachydactylus* geckos. BMC Evol. Biol. 17:9.
702 Hipsley, C. A., D. B. Miles, and J. Muller. 2014. Morphological disparity opposes latitudinal
703 diversity gradient in lacertid lizards. Biol. Lett. 10:20140101.
704 Hutchinson, M. N., M. J. Sistrom, S. C. Donnellan, and R. G. Hutchinson. 2014. Taxonomic
705 revision of the Australian arid zone lizards *Gehyra variegata* and *G. montium*
706 (Squamata, Gekkonidae) with description of three new species. Zootaxa 3814:221–
707 241.

Jetz, W., G. H. Thomas, J. B. Joy, K. Hartmann, and A. O. Mooers. 2012. The global diversity of birds in space and time. Nature 491:444–448.

Jones, M. R. and J. M. Good. 2016. Targeted capture in evolutionary and ecological genomics. Mol. Ecol. 25:185–202.

Kealley, L., P. Doughty, M. Pepper, S. Keogh, M. Hillier, and J. Huey. in press. Conspicuously concealed: revision of the arid clade of the *Gehyra variegata* (Gekkonidae) species group in Western Australia using an integrative molecular and morphological approach, with the description of five cryptic species. PeerJ.

Kembel, S. W., P. D. Cowan, M. R. Helmus, W. K. Cornwell, H. Morlon, D. D. Ackerly, S. P. Blomberg, and C. O. Webb. 2010. Picante: R tools for integrating phylogenies and ecology. Bioinformatics 26:1463–1464.

King, M. 1979. Karyotypic evolution in *Gehyra* (Gekkonidae: Reptilia) I. The *Gehyra variegata-punctata* complex. Aust. J. Zool. 27:323–343.

Kozak, K. H., D. W. Weisrock, and A. Larson. 2006. Rapid lineage accumulation in a non-adaptive radiation: phylogenetic analysis of diversification rates in eastern North American woodland salamanders (Plethodontidae: *Plethodon*). Proc. R. Soc. B 273:539–546.

Kück, P. and K. Meusemann. 2010. FASconCAT: convenient handling of data matrices. Mol. Phylogen. Evol. 56:1115–1118.

Lack, D. 1947. Darwin's finches. Cambridge University Press, London.

Landis, M. J., N. J. Matzke, B. R. Moore, and J. P. Huelsenbeck. 2013. Bayesian analysis of biogeography when the number of areas is large. Syst. Biol. 62:789–804.

Laver, R. J., P. Doughty, and P. M. Oliver. 2017. Origins and patterns of endemic diversity in two specialized lizard lineages from the Australian Monsoonal Tropics (*Oedura* spp.). J. Biogeogr. doi: 10.1111/jbi.13127.

733 Leaché, A. D. and M. K. Fujita. 2010. Bayesian species delimitation in West African forest
734 geckos (*Hemidactylus fasciatus*). Proc. R. Soc. B 277:3071–3077.
735 Lewis, P. O. 2001. A likelihood approach to estimating phylogeny from discrete
736 morphological character data. Syst. Biol. 50:913–925.
737 Losos, J. B. 2009. Lizards in an evolutionary tree: ecology and adaptive radiation of anoles.
738 University of California Press, Berkeley.
739 Losos, J. B., R. E. Glor, J. J. Kolbe, and K. Nicholson. 2006. Adaptation, speciation, and
740 convergence: a hierarchical analysis of adaptive radiation in Caribbean *Anolis* lizards.
741 Ann. Mo. Bot. Gard. 93:24–33.
742 Martin, H. A. 2006. Cenozoic climatic change and the development of the arid vegetation in
743 Australia. J. Arid Environ. 66:533–563.
744 Matzke, N. J. 2013a. BioGeoBEARS: BioGeography with Bayesian (and likelihood)
745 Evolutionary Analysis in R Scripts. University of California, Berkeley, Berkeley, CA.
746 Available at http://cran.r-project.org/package=BioGeoBEARS.
747 Matzke, N. J. 2013b. Probabilistic historical biogeography: new models for founder-event
748 speciation, imperfect detection, and fossils allow improved accuracy and model-
749 testing. Front. Biogeogr. 5:242–248.
750 Matzke, N. J. 2014. Model selection in historical biogeography reveals that founder-event
751 speciation is a crucial process in island clades. Syst. Biol. 63:951–970.
752 Matzke, N. J. 2015. BEASTmasteR: automated conversion of NEXUS data to BEAST2 XML
753 format, for fossil tip-dating and other uses. PhyloWiki. Available at
754 http://phylo.wikidot.com/beastmaster.
755 Matzke, N. J. and A. M. Wright. 2016. Inferring node dates from tip dates in fossil Canidae:
756 the importance of tree priors. Biol. Lett. 12:20160328.

Mirarab, S. and T. Warnow. 2015. ASTRAL-II: coalescent-based species tree estimation with many hundreds of taxa and thousands of genes. Bioinformatics 31:i44–i52.

Mitchell, F. J. 1965. Australian geckos assigned to the genus *Gehyra* Gray (Reptilia, Gekkonidae). Senckenb. Biol. 46:287–319.

Moritz, C., J. L. Patton, C. J. Schneider, and T. B. Smith. 2000. Diversification of rainforest faunas: an integrated molecular approach. Annu. Rev. Ecol. Syst. 31:533–563.

Moritz, C., R. C. Pratt, S. Bank, G. Bourke, J. G. Bragg, P. Doughty, J. S. Keogh, R. J. Laver, S. Potter, L. C. Teasdale, L. G. Tedeschi, and P. M. Oliver. 2018. Cryptic lineage diversity, body size divergence and sympatry in a species complex of Australian lizards (*Gehyra*). Evolution 72:54–66.

Moritz, C. M. 1986. The population biology of *Gehyra* (Gekkonidae): chromosome change and speciation. Systematic Zoology 35:46–67.

Moritz, C. M. 1992. The population biology of *Gehyra* (Gekkonidae). III. Patterns of microgeographic variation. J. Evol. Biol. 5:661–676.

Morton, S. R., J. Short, and R. D. Barker. 1995. Refugia for Biological Diversity in Arid and Semi-arid Australia: a Report to the Biodiversity Unit of the Department of Environment, Sport and Territories. Dept. of Environment, Sport and Territories, Canberra.

Nguyen, L. T., H. A. Schmidt, A. von Haeseler, and B. Q. Minh. 2015. IQ-TREE: a fast and effective stochastic algorithm for estimating maximum-likelihood phylogenies. Mol. Biol. Evol. 32:268–274.

Ogilvie, H. A., R. Bouckaert, and A. J. Drummond. 2017. StarBEAST2 brings faster species tree inference and accurate estimates of substitution rates. Mol. Biol. Evol. 34:2101–2114.

781 Ogilvie, H. A., J. Heled, D. Xie, and A. J. Drummond. 2016. Computational performance and
782 statistical accuracy of *BEAST and comparisons with other methods. Syst. Biol.
783 65:381–396.
784 Oliver, P. M., M. Adams, and P. Doughty. 2010. Molecular evidence for ten species and
785 Oligo-Miocene vicariance within a nominal Australian gecko species (*Crenadactylus*
786 *ocellatus*, Diplodactylidae). BMC Evol. Biol. 10:386.
787 Oliver, P. M. and A. M. Bauer. 2011. Systematics and evolution of the Australian knob-tail
788 geckos (*Nephrurus*, Carphodactylidae, Gekkota): Plesiomorphic grades and biome
789 shifts through the Miocene. Mol. Phylogen. Evol. 59:664–674.
790 Oliver, P. M., G. Bourke, R. C. Pratt, P. Doughty, and C. Moritz. 2016. Systematics of small
791 *Gehyra* (Squamata: Gekkonidae) of the southern Kimberley, Western Australia:
792 redescription of *G. kimberleyi* Borner & Schuttler, 1983 and description of a new
793 restricted range species. Zootaxa 4107:49–64.
794 Oliver, P. M., P. J. Couper, and M. Pepper. 2014a. Independent transitions between
795 monsoonal and arid biomes revealed by systematic revison of a complex of Australian
796 geckos (*Diplodactylus*; Diplodactylidae). PLOS ONE 9:e111895.
797 Oliver, P. M., R. J. Laver, F. De Mello Martins, R. C. Pratt, S. Hunjan, and C. C. Moritz.
798 2017. A novel hotspot of vertebrate endemism and an evolutionary refugium in
799 tropical Australia. Divers. Distrib. 23:53–66.
800 Oliver, P. M. and P. J. McDonald. 2016. Young relicts and old relicts: a novel palaeoendemic
801 vertebrate from the Australian Central Uplands. R. Soc. Open Sci. 3:160018.
802 Oliver, P. M., P. Skipwith, and M. S. Y. Lee. 2014b. Crossing the line: increasing body size
803 in a trans-Wallacean lizard radiation (*Cyrtodactylus*, Gekkota). Biol. Lett.
804 10:20140479.

Oliver, P. M., K. L. Smith, R. J. Laver, P. Doughty, M. Adams, and B. Riddle. 2014c. Contrasting patterns of persistence and diversification in vicars of a widespread Australian lizard lineage (the *Oedura marmorata* complex). J. Biogeogr. 41:2068–2079.

Orme, D. 2013. Caper: Comparative analyses of phylogenetics and evolution in R. Available at http://cran.r-project.org/web/packages/caper/vignettes/caper.pdf.

Paradis, E., J. Claude, and K. Strimmer. 2004. APE: analyses of phylogenetics and evolution in R language. Bioinformatics 20:289–290.

Pattengale, N. D., M. Alipour, O. R. Bininda-Emonds, B. M. Moret, and A. Stamatakis. 2010. How many bootstrap replicates are necessary? J. Comput. Biol. 17:337–354.

Peñalba, J. V., L. L. Smith, M. A. Tonione, C. Sass, S. M. Hykin, P. L. Skipwith, J. A. McGuire, R. C. K. Bowie, and C. Moritz. 2014. Sequence capture using PCR-generated probes: a cost-effective method of targeted high-throughput sequencing for nonmodel organisms. Mol. Ecol. Resour. 14:1000–1010.

Pennell, M. W., J. M. Eastman, G. J. Slater, J. W. Brown, J. C. Uyeda, R. G. FitzJohn, M. E. Alfaro, and L. J. Harmon. 2014. geiger v2.0: an expanded suite of methods for fitting macroevolutionary models to phylogenetic trees. Bioinformatics 30:2216–2218.

Pepper, M., P. Doughty, and J. S. Keogh. 2013. Geodiversity and endemism in the iconic Australian Pilbara region: a review of landscape evolution and biotic response in an ancient refugium. J. Biogeogr. 40:1225–1239.

Pepper, M., M. K. Fujita, C. Moritz, and J. S. Keogh. 2011. Palaeoclimate change drove diversification among isolated mountain refugia in the Australian arid zone. Mol. Ecol. 20:1529–1545.

Pérez-Ponce de León, G. and R. Poulin. 2016. Taxonomic distribution of cryptic diversity among metazoans: not so homogeneous after all. Biol. Lett. 12:20160371.

Pianka, E. R. and H. D. Pianka. 1976. Comparative ecology of twelve species of nocturnal lizards (Gekkonidae) in the Western Australian desert. Copeia 1976:125–142.

Pinheiro, J., D. Bates, S. DebRoy, D. Sarkar, and R Core Team. 2015. nlme: Linear and Nonlinear Mixed Effects models. Available at http://cran.r-project.org/package=nlme.

Poe, S., A. N.-M. de Oca, O. Torres-Carvajal, K. de Queiroz, J. A. Velasco, B. Truett, L. N. Gray, M. J. Ryan, G. Köhler, F. Ayala-Varela, and I. Latella. 2018. Comparative evolution of an archetypal adaptive radiation: innovation and opportunity in *Anolis* lizards. Am. Nat. 191:E000–E000.

Purvis, A. 2008. Phylogenetic approaches to the study of extinction. Annu. Rev. Ecol. Evol. Syst. 39:301–319.

R Core Development Team. 2015. R: a language and environment for statistical computing. R Foundation for Statistical Computing, Vienna, Austria. Available at http://www.r-project.org/.

Rabosky, D. L., S. C. Donnellan, M. Grundler, and I. J. Lovette. 2014. Analysis and visualization of complex macroevolutionary dynamics: an example from Australian scincid lizards. Syst. Biol. 63:610–627.

Ranwez, V., S. Harispe, F. Delsuc, and E. J. P. Douzery. 2011. MACSE: Multiple Alignment of Coding SEquences accounting for frameshifts and stop codons. PLOS ONE 6:e22594.

Ree, R. H., S. A. Smith, and A. Baker. 2008. Maximum likelihood inference of geographic range evolution by dispersal, local extinction, and cladogenesis. Syst. Biol. 57:4–14.

Revell, L. J. 2012. Phytools: an R package for phylogenetic comparative biology (and other things). Methods Ecol. Evol. 3:217–223.

853 Revell, L. J., M. A. Johnson, J. A. Schulte, 2nd, J. J. Kolbe, and J. B. Losos. 2007. A
854 phylogenetic test for adaptive convergence in rock-dwelling lizards. Evolution
855 61:2898–2912.
856 Ronquist, F. 1997. Dispersal-vicariance analysis: a new approach to the quantification of
857 historical biogeography. Syst. Biol. 46:195–203.
858 Rundell, R. J. and T. D. Price. 2009. Adaptive radiation, nonadaptive radiation, ecological
859 speciation and nonecological speciation. Trends Ecol. Evol. 24:394–399.
860 Schluter, D. 2000. The ecology of adaptive radiation. Oxford University Press, Oxford.
861 Singhal, S. 2013. De novo transcriptomic analyses for non-model organisms: an evaluation of
862 methods across a multi-species data set. Mol. Ecol. Resour. 13:403–416.
863 Singhal, S. and C. Moritz. 2013. Reproductive isolation between phylogeographic lineages
864 scales with divergence. Proc. R. Soc. B 280:20132246.
865 Sistrom, M., S. C. Donnellan, and M. N. Hutchinson. 2013. Delimiting species in recent
866 radiations with low levels of morphological divergence: a case study in Australian
867 *Gehyra* geckos. Mol. Phylogen. Evol. 68:135–143.
868 Sistrom, M., D. L. Edwards, S. Donnellan, and M. Hutchinson. 2012. Morphological
869 differentiation correlates with ecological but not with genetic divergence in a *Gehyra*
870 gecko. J. Evol. Biol. 25:647–660.
871 Sistrom, M., M. Hutchinson, T. Bertozzi, and S. Donnellan. 2014. Evaluating evolutionary
872 history in the face of high gene tree discordance in Australian *Gehyra* (Reptilia:
873 Gekkonidae). Heredity 113:52–63.
874 Sistrom, M. J., M. N. Hutchinson, R. G. Hutchinson, and S. C. Donnellan. 2009. Molecular
875 phylogeny of Australian *Gehyra* (Squamata: Gekkonidae) and taxonomic revision of
876 *Gehyra variegata* in south-eastern Australia. Zootaxa 2277:14–32.

877 Smith, B. T., J. E. McCormack, A. M. Cuervo, M. J. Hickerson, A. Aleixo, C. D. Cadena, J.
878 Pérez-Emán, C. W. Burney, X. Xie, M. G. Harvey, B. C. Faircloth, T. C. Glenn, E. P.
879 Derryberry, J. Prejean, S. Fields, and R. T. Brumfield. 2014. The drivers of tropical
880 speciation. Nature 515:406–409.
881 Sniderman, J. M., J. D. Woodhead, J. Hellstrom, G. J. Jordan, R. N. Drysdale, J. J. Tyler, and
882 N. Porch. 2016. Pliocene reversal of late Neogene aridification. Proc. Natl. Acad. Sci.
883 USA 113:1999–2004.
884 Stamatakis, A. 2014. RAxML version 8: a tool for phylogenetic analysis and post-analysis of
885 large phylogenies. Bioinformatics 30:1312–1313.
886 Stayton, C. T. 2005. Morphological evolution of the lizard skull: a geometric morphometrics
887 survey. J. Morphol. 263:47–59.
888 Storr, G. M., L. A. Smith, and R. E. Johnstone. 1990. Lizards of Western Australia III:
889 geckos and pygopods. Western Australian Museum, Perth.
890 Struck, T. H., J. L. Feder, M. Bendiksby, S. Birkeland, J. Cerca, V. I. Gusarov, S. Kistenich,
891 K.-H. Larsson, L. H. Liow, M. D. Nowak, B. Stedje, L. Bachmann, and D. Dimitrov.
892 2018. Finding evolutionary processes hidden in cryptic species. Trends Ecol. Evol.
893 33:153–163.
894 Sukumaran, J. and L. L. Knowles. 2017. Multispecies coalescent delimits structure, not
895 species. Proceedings of the National Academy of Sciences 114:1607–1612.
896 Tonione, M. A., R. N. Fisher, C. Zhu, and C. Moritz. 2016. Deep divergence and structure in
897 the Tropical Oceanic Pacific: a multilocus phylogeography of a widespread gekkonid
898 lizard (Squamata: Gekkonidae: *Gehyra oceanica*). J. Biogeogr. 43:268–278.
899 Vitt, L. J., P. A. Caldwell, P. Zani, and T. A. Titus. 1997. The role of habitat shift in the
900 evolution of lizards morphology: evidence from tropical Tropidurines. Proc. Natl.
901 Acad. Sci. USA 94:3828–3832.

902 Wilson, S. and G. Swan. 2013. A complete guide to reptiles of Australia. New Holland
903 Publishers, Australia.
904 Yang, Z. 2015. The BPP program for species tree estimation and species delimitation. Curr.
905 Zool. 61:854–865.
906 Yoder, J. B., E. Clancey, S. Des Roches, J. M. Eastman, L. Gentry, W. Godsoe, T. J. Hagey,
907 D. Jochimsen, B. P. Oswald, J. Robertson, B. A. J. Sarver, J. J. Schenk, S. F. Spear,
908 and L. J. Harmon. 2010. Ecological opportunity and the origin of adaptive radiations.
909 J. Evol. Biol. 23:1581–1596.

910

Table 1 Mean rates of diversification and morphological evolution of the *Gehyra variegata* group estimated using the StarBEAST2 species tree.

Grouping	DR statistic (lineages/My) with 95% CI	Morphological evolution rate (σ^2/My)
variegata group	0.301 (0.133–0.626)	N/A
AMT taxa	0.231 (0.136–0.349)	9.14E-5
Central AAZ taxa	0.377 (0.104–0.676)	1.84E-4
Pilbara taxa	0.312 (0.146–0.491)	1.11E-4
Rock-dwellers	0.281 (0.125–0.545)	1.14E-4
Generalists	0.375 (0.144–0.676)	1.41E-4

Figure legends

Fig. 1 Locations of *Gehyra variegata* group samples used for exon capture phylogenomics (listed in Table S1). The top left pane shows Australia, with the Australian monsoonal tropics (AMT) and Australian arid zone (AAZ) biomes coloured blue and orange, respectively. Panes 1–3 zoom in on western, northern, and southern Australia, with the *Gehyra* samples coloured by lineage (as per the key on the right).

Fig. 2 *Gehyra* phylogenies inferred using (A) RAxML concatenation of 547 loci, and (B) ASTRAL summary species tree method with 499 loci. Branch supports are maximum likelihood bootstrap values, and the RAxML scale bar is nucleotide sequence change per My. The RAxML tree is coloured by habitat type and main clades are labelled as follows: (i) *lazelli-pulingka* (AAZ), (ii) *nana* clade (AMT), and (iii) an AAZ clade containing *G. moritzi* and the main AAZ clade, which itself has five groups: (a) *purpurascens-einasleighensis*, (b) *variegataC1-2*, (c) the *punctata B* clade, (d) the *punctata A* clade, and (e) the *variegata* clade.

928 **Fig. 3** *Gehyra* phylogeny inferred using StarBEAST2 species tree method with 106 loci,
929 calibrated with a root age of 19.1 Mya. Branch supports are posterior probabilities, node bars
930 show 95% highest posterior density of node age and the scale bar is millions of years ago.
931 Main clades are labelled as follows: *variegata* group (ingroup), (ii) *nana* clade (AMT), and
932 (iii) an AAZ clade containing *G. moritzi*, (i) *lazelli-pulingka*, and the main AAZ clade, which
933 itself has six groups: (a) *purpurascens-einasleighensis*, (b.1) *variegataC2*, (c) the *punctata B*
934 clade, (b.2) *variegataC1*, (d) the *punctata A* clade, and (e) the *variegata* clade.

935 **Fig. 4** *Gehyra variegata* group ancestral state estimation analyses using BioGeoBEARS,
936 under the best-fitting model on the StarBEAST2 species tree. Scale bars are in Mya. (A)
937 Geographic range analysis under the DEC model: the AMT is blue, the central AAZ is
938 orange, and the Pilbara (western AAZ) is red. (B) Biome analysis under the M*k* model: the
939 AMT is blue and the AAZ is orange. (C) Habitat analysis under the M*k* model: rock-dwelling
940 is red and generalist is green.

941 **Fig. 5** Phylomorphospace plots showing divergence in body shape (A–C: rPC1–3, head and
942 foreleg dimensions) against body size (log SVL). *Gehyra* lineages are coloured by habitat
943 type (red = rock-dwellers, green = generalists), with the StarBEAST2 phylogeny as
944 connecting lines. (A) Three pairs of lineages are circled in orange (small-bodied on the left,
945 large-bodied on the right) to highlight the body size disparity within the *purpurascens-*
946 *einasleighensis* clade, the *nana* clade (*G. granulum* vs. *G. occidentalis*), and the *punctata B*
947 clade (*G. punctataB1* vs. *G. punctataB3*). The termite mound specialist *G. pilbara* is circled
948 in blue to highlight its unusually short head.

949 **Fig. 6** Divergence of size-corrected (A) snout depth and (B) head depth between rock-
950 dwelling and generalist *Gehyra* lineages. Asterisks indicate statistical significance (*p* value
951 0.01–0.001).

952

953

954 **Supplementary Methods, Results, Figures, Tables:** see Supporting Information file

955

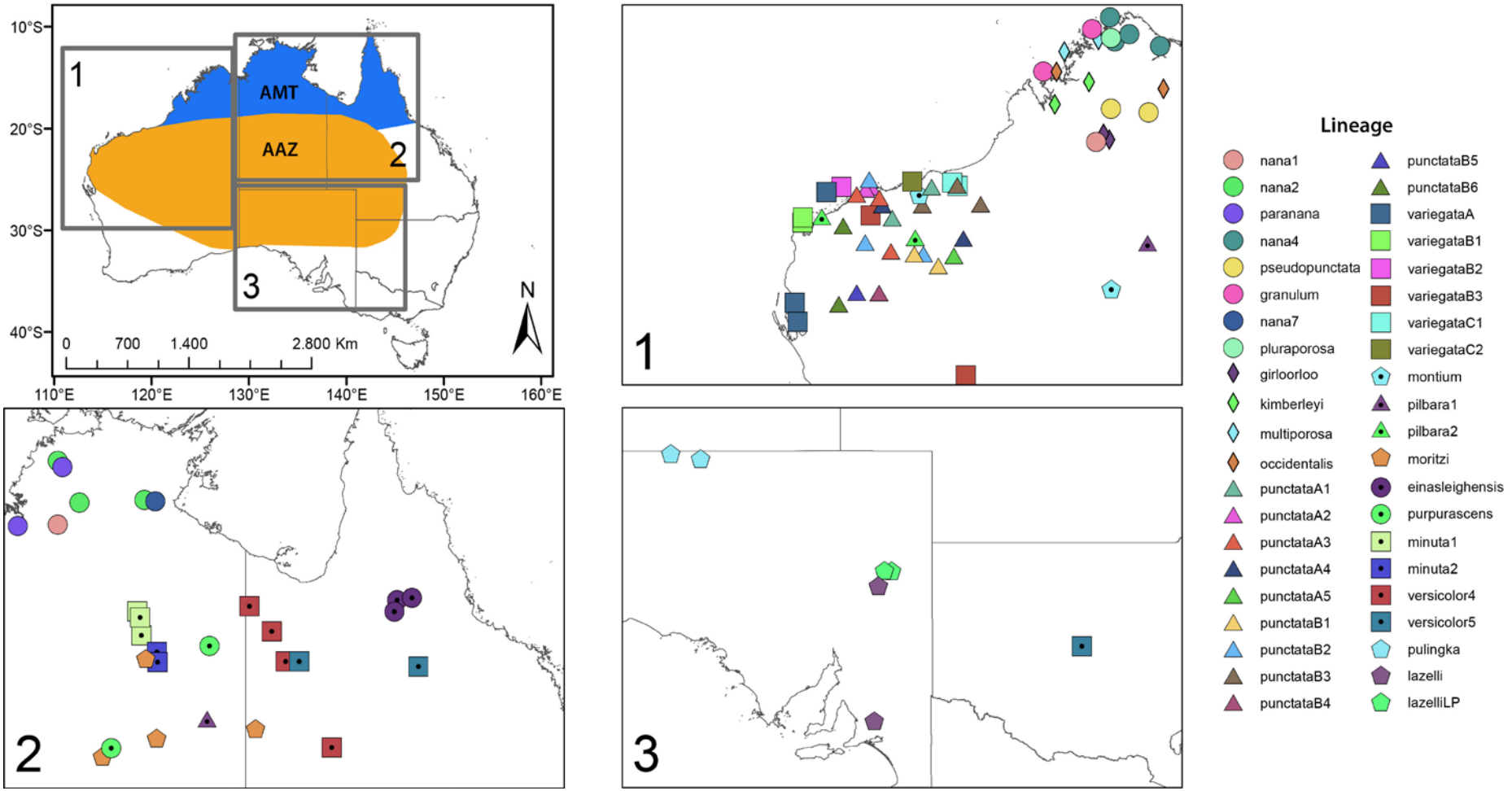
10°S
20°S
30°S
40°S
110°E
120°E
130°E
140°E
150°E
160°E
1
2
3
AMT
AAZ
0
700
1.400
2.800 Km
N
Lineage
nana1
nana2
paranana
nana4
pseudopunctata
granulum
nana7
pluraporosa
girloorloo
kimberleyi
multiporosa
occidentalis
punctataA1
punctataA2
punctataA3
punctataA4
punctataA5
punctataB1
punctataB2
punctataB3
punctataB4
punctataB5
punctataB6
variegataA
variegataB1
variegataB2
variegataB3
variegataC1
variegataC2
montium
pilbara1
pilbara2
moritzi
einasleighensis
purpurascens
minuta1
minuta2
versicolor4
versicolor5
pulingka
lazelli
lazelliLP

956

957

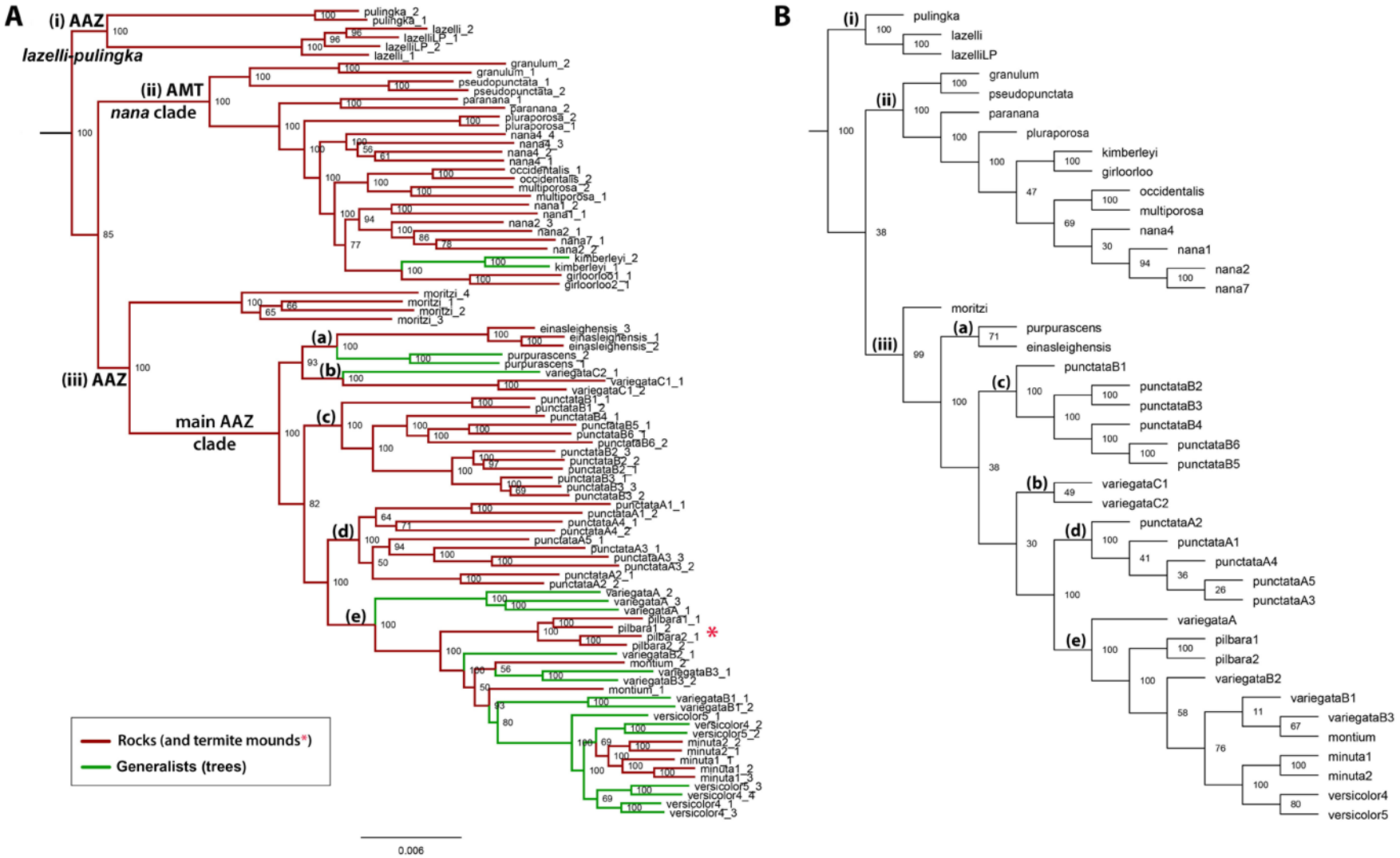
A
(i) AAZ
lazelli-pulingka
(ii) AMT
nana clade
(iii) AAZ
main AAZ
clade
(a)
(b)
(c)
(d)
(e)
Rocks (and termite mounds*)
Generalists (trees)
0.006
B
(i)
(ii)
(iii)
pulingka
lazelli
lazelliLP
granulum
pseudopunctata
paranana
pluraporosa
kimberleyi
girloorloo
occidentalis
multiporosa
nana4
nana1
nana2
nana7
moritzi
purpurascens
einasleighensis
punctataB1
punctataB2
punctataB3
punctataB4
punctataB6
punctataB5
variegataC1
variegataC2
punctataA2
punctataA1
punctataA4
punctataA5
punctataA3
variegataA
pilbara1
pilbara2
variegataB2
variegataB1
variegataB3
montium
minuta1
minuta2
versicolor4
versicolor5

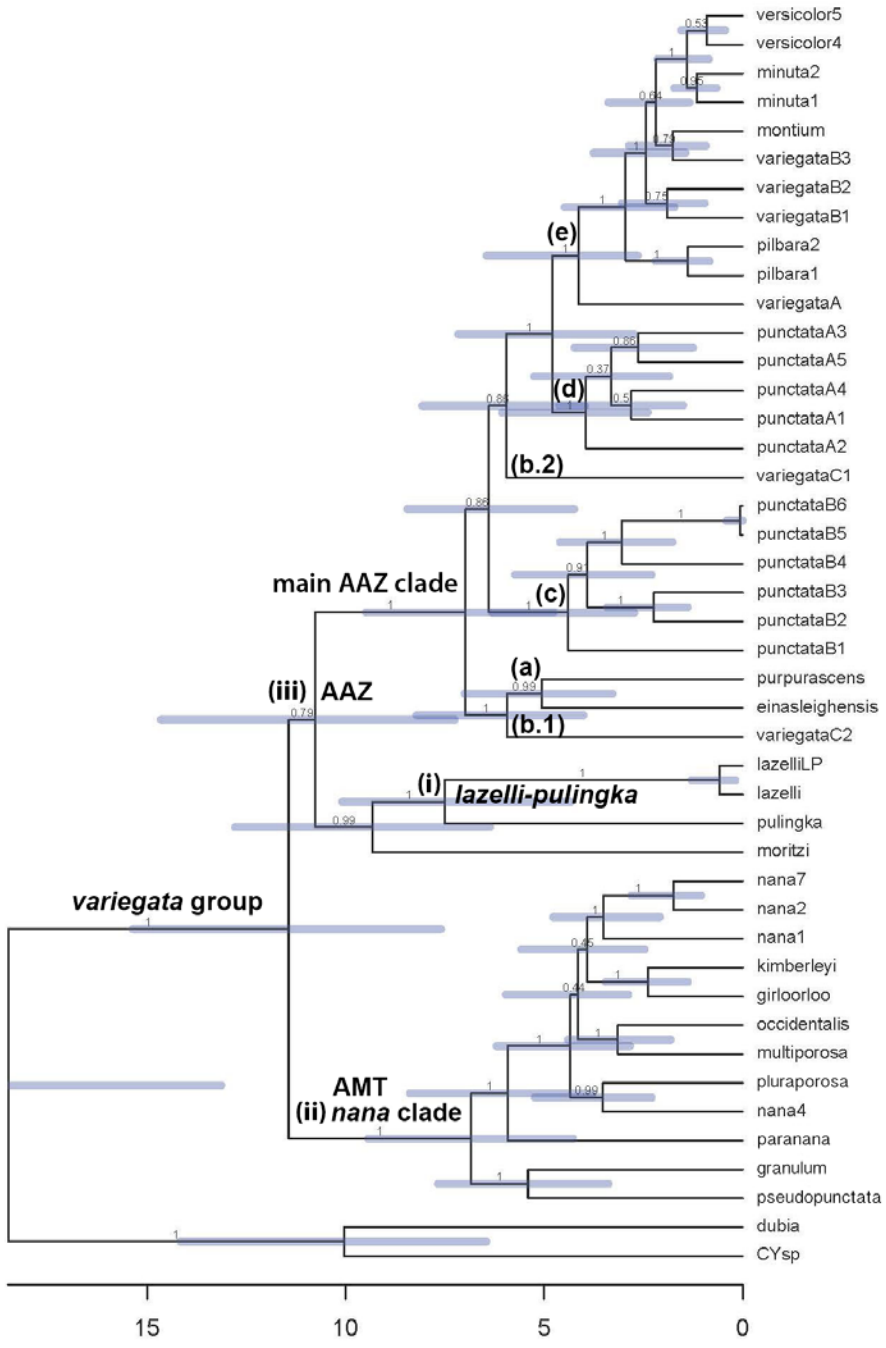
versicolor5
versicolor4
minuta2
minuta1
montium
variegataB3
variegataB2
variegataB1
(e)
pilbara2
pilbara1
variegataA
punctataA3
punctataA5
(d)
punctataA4
punctataA1
punctataA2
(b.2)
variegataC1
punctataB6
punctataB5
punctataB4
main AAZ clade
(c)
punctataB3
punctataB2
punctataB1
(a)
purpurascens
(iii) AAZ
einasleighensis
(b.1)
variegataC2
lazelliLP
(i) lazelli-pulingka
lazelli
pulingka
moritzi
variegata group
nana7
nana2
nana1
kimberleyi
girloorloo
occidentalis
multiporosa
AMT
(ii) nana clade
pluraporosa
nana4
paranana
granulum
pseudopunctata
dubia
CYsp
15
10
5
0

960

961

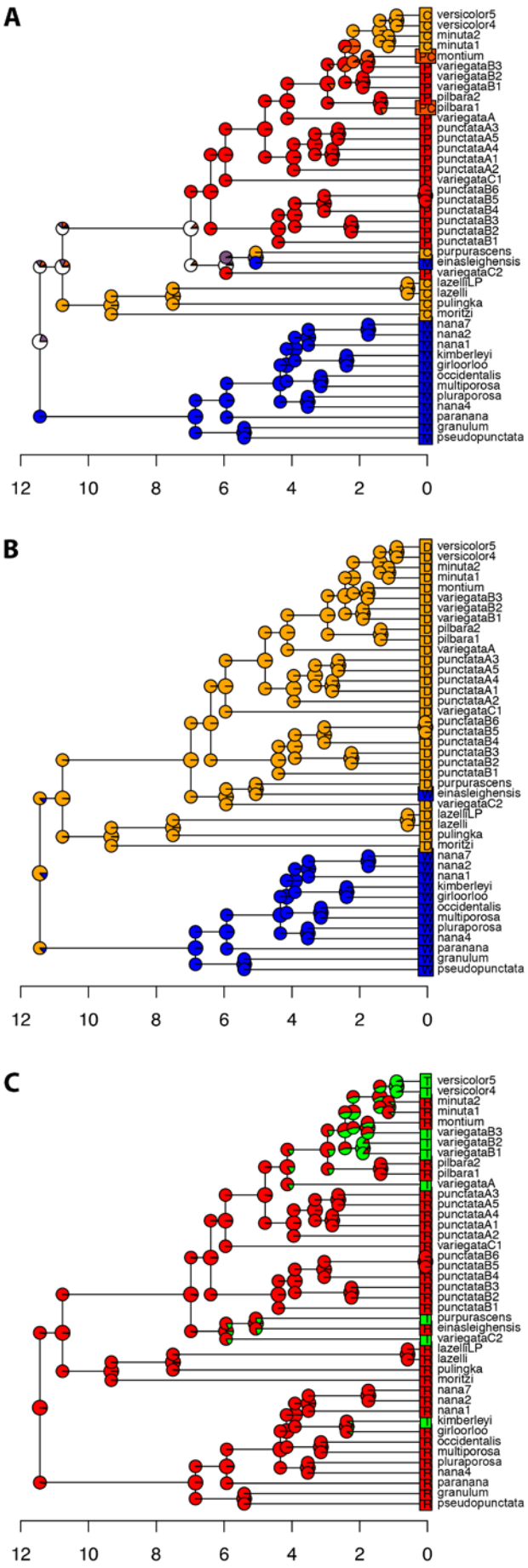
A
versicolor5
versicolor4
minuta2
minuta1
montium
variegataB3
variegataB2
variegataB1
pilbara2
pilbara1
variegataA
punctataA3
punctataA5
punctataA4
punctataA1
punctataA2
variegataC1
punctataB6
punctataB5
punctataB4
punctataB3
punctataB2
punctataB1
purpurascens
einasleighensis
variegataC2
lazelliLP
lazelli
pulingka
moritzi
nana7
nana2
nana1
kimberleyi
girloorloo
occidentalis
multiporosa
pluraporosa
nana4
paranana
granulum
pseudopunctata
12
10
8
6
4
2
0
B
versicolor5
versicolor4
minuta2
minuta1
montium
variegataB3
variegataB2
variegataB1
pilbara2
pilbara1
variegataA
punctataA3
punctataA5
punctataA4
punctataA1
punctataA2
variegataC1
punctataB6
punctataB5
punctataB4
punctataB3
punctataB2
punctataB1
purpurascens
einasleighensis
variegataC2
lazelliLP
lazelli
pulingka
moritzi
nana7
nana2
nana1
kimberleyi
girloorloo
occidentalis
multiporosa
pluraporosa
nana4
paranana
granulum
pseudopunctata
12
10
8
6
4
2
0
C
versicolor5
versicolor4
minuta2
minuta1
montium
variegataB3
variegataB2
variegataB1
pilbara2
pilbara1
variegataA
punctataA3
punctataA5
punctataA4
punctataA1
punctataA2
variegataC1
punctataB6
punctataB5
punctataB4
punctataB3
punctataB2
punctataB1
purpurascens
einasleighensis
variegataC2
lazelliLP
lazelli
pulingka
moritzi
nana7
nana2
nana1
kimberleyi
girloorloo
occidentalis
multiporosa
pluraporosa
nana4
paranana
granulum
pseudopunctata
12
10
8
6
4
2
0

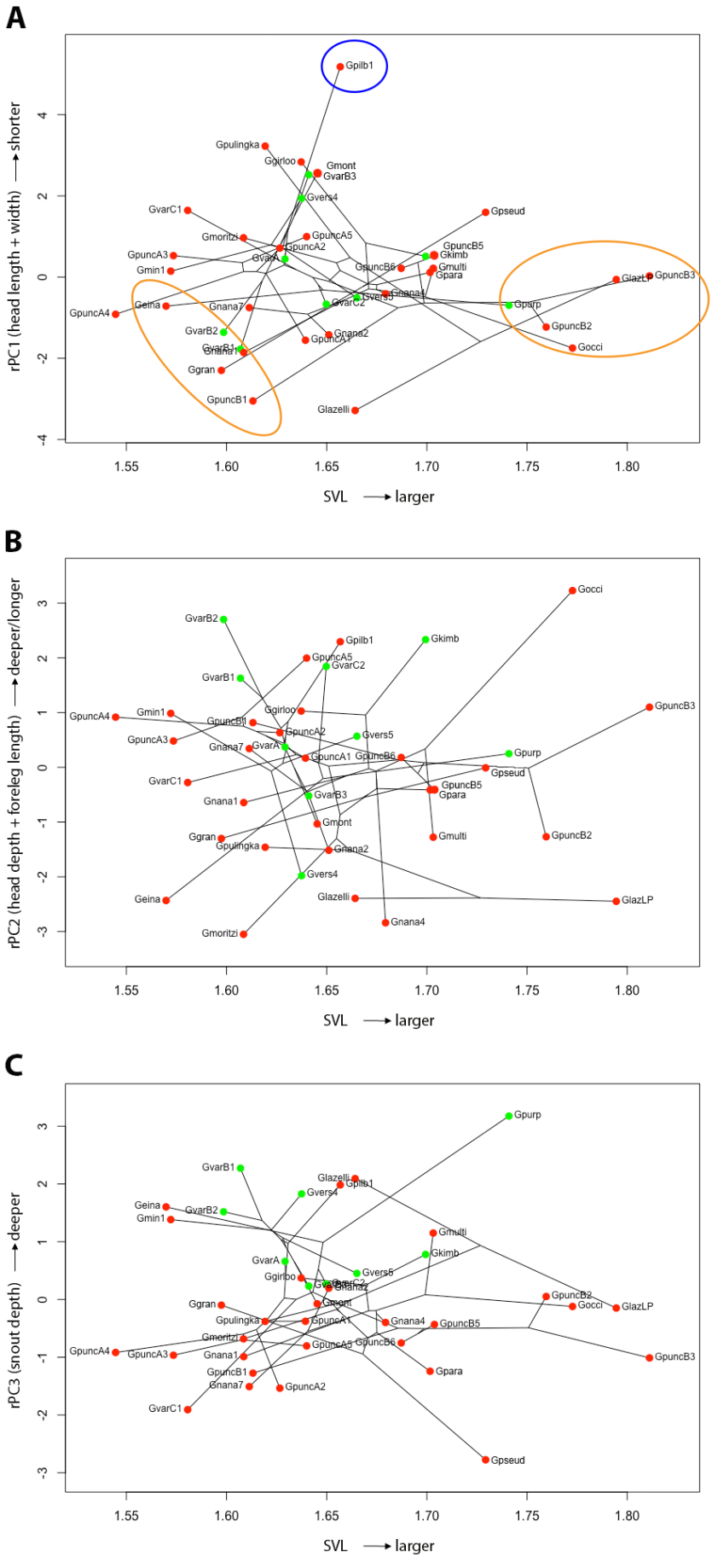
A
rPC1 (head length + width) ⟶ shorter
SVL ⟶ larger
B
rPC2 (head depth + foreleg length) ⟶ deeper/longer
SVL ⟶ larger
C
rPC3 (snout depth) ⟶ deeper
SVL ⟶ larger

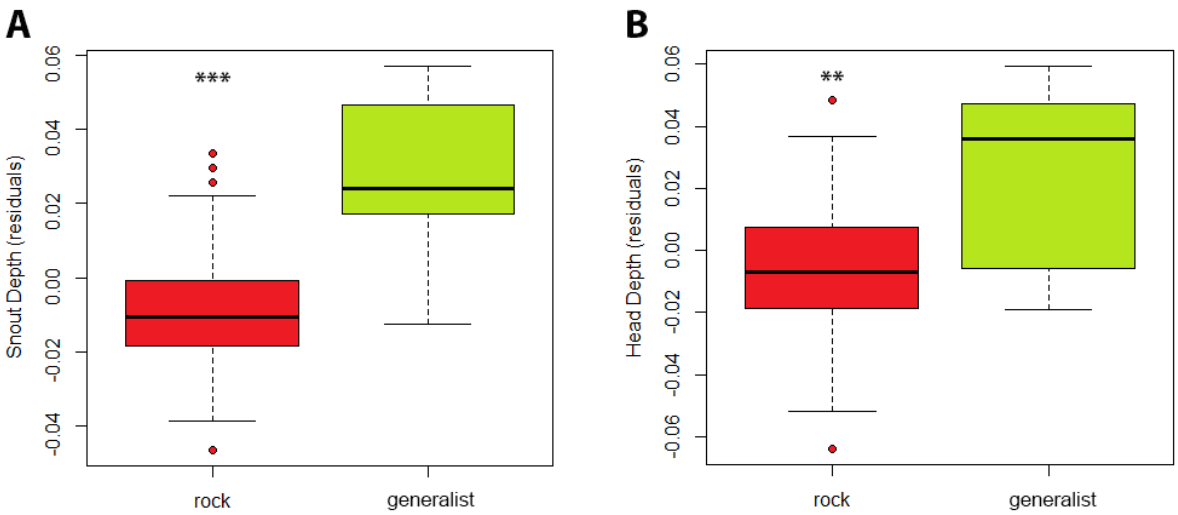
A
Snout Depth (residuals)
0.06
0.04
0.02
0.00
-0.02
-0.04
***
rock
generalist
B
Head Depth (residuals)
0.06
0.04
0.02
0.00
-0.02
-0.04
-0.06
**
rock
generalist

964